Picosecond laser ablation mechanism of CVD diamond

Zhang Quanli[1,#], Xu Boxin[1], Fu Yucan[1]

1 College of Mechanical and Electrical Engineering, Nanjing University of Aeronautics and Astronautics, Nanjing 210016, China
Corresponding Author / Email: zhangql@nuaa.edu.cn , TEL: +86-02584890644

KEYWORDS: CVD diamond, Picosecond laser, Two-temperature model, Molecular dynamics

CVD diamond is of excellent mechanical and optical properties to make it widely applied in the field of microelectronics and optical devices. To achieve efficient and precise processing of CVD diamond, the use of ultrashort pulse laser processing of CVD diamond is an effective method. In this paper, based on the interaction theory between ultrashort pulsed laser and CVD diamond, the changes of absorption coefficient and reflectivity of diamond surface during picosecond laser ablation are taken into consideration, and the two-temperature model are improved to couple with molecular dynamics. The mechanism of picosecond laser ablation of CVD diamond was then investigated, where the temporal evolution of free electron density, electron temperature and lattice temperature on CVD diamond were analyzed and the process of picosecond laser ablation of CVD diamond was simulated. Finally, the built model was verified by the ablation experiment, where the ablation threshold and the achieved surface characteristics are involved.

1. Introduction

CVD diamond is a typical hard and brittle material with excellent mechanical and optical properties such as high hardness, high wear resistance and high refractive index [1-4], which has a wide range of applications in the field of microelectronics and optical devices [5-7]. However, the extremely high hardness of diamond makes processing difficult, and traditional processing methods such as EDM cutting and grinding have problems such as low processing efficiency [8], and laser processing has the characteristics of short processing time and high processing efficiency, which is an effective method for processing diamond.

The interaction between ultrashort pulsed laser and diamond is a nonlinear, multiscale and complex process, which includes photon energy absorption, free-electron excitation, electron-phonon coupling, plasma excitation and expansion, and the time of action is often around picoseconds. In order to elucidate the interaction mechanism between ultrashort pulsed laser and diamond, a lot of theoretical and experimental laser processing of diamond have been carried out in the past studies [9-12]. The two-temperature model was proposed by Anisimov et al [13] in 1974, which can well describe the electron-phonon coupling and temperature equilibrium process during the interaction between the ultrashort-pulse laser and the metal.Jiang et al [14] improved the two-temperature model, and successfully predicted the ablation threshold of the femtosecond laser ablation of the gold film. However, semiconductor materials such as diamond are different from metals, and the traditional two-temperature model cannot describe the free electron density change caused by the valence band electrons jumping to the conduction band after diamond is irradiated by the laser, and it needs to be corrected by adding the photoionisation equation describing the change of the free electron density on the basis of the two-temperature model. Yin et al [15] used the photoionization equation to describe the evolution of free electron density during femtosecond laser ablation of single-crystal diamond and established a two-temperature model for the variation of surface reflectance and absorption coefficient with free electron density, and the results showed that the improved two-temperature model could successfully predict the ablation threshold of femtosecond laser ablation of single-crystal diamond, and the prediction results were in agreement with the experimental results.

Molecular dynamics is a comprehensive simulation method combining classical mechanics, materials science and other basic theories. Molecular dynamics simulation can simulate the evolution process of materials at the microscopic scale and within a very short time, so it is suitable for studying the interaction mechanism between ultrashort pulsed lasers and materials. Cui et al [16] investigated the process of laser ablation of CVD diamond using molecular dynamics simulation, and the results showed that the graphite layer of CVD diamond with smaller grain size was thicker after laser ablation. Tian et al [17] established a molecular dynamics model describing nanosecond laser ablation of diamond to analyze the correlation between temperature distribution and ablation phenomena, and investigated the causes of dislocations within diamond during laser ablation, which showed that the stress wave plays an important role in the formation and propagation of dislocations, and that the speed of the stress wave and the rate of cooling down of polycrystalline diamond are both slower than those of single-crystalline diamond after laser ablation. Liu et al [18] coupled the two-temperature model with the molecular dynamics to study the ablation mechanism of picosecond laser ablation ablation of monocrystalline silicon, and it was shown that, with the increase of the laser energy density , the material removal mechanism

changes from evaporation to molten liquid sputtering and finally to phase explosion.

In this study, a model coupling the two-temperature model and molecular dynamics was established to study the ablation mechanism of picosecond laser ablation of CVD diamond.The improved two-temperature model describes the process of electron-phonon coupling in diamond during laser ablation, the ablation threshold of picosecond laser ablation of CVD diamond is calculated, and the ablation mechanism of picosecond laser ablation of CVD diamond is investigated by molecular dynamics simulation, and finally the simulation results are verified by the ablation threshold test.

2. Theoretical model

2.1 Two-temperature model

As mentioned earlier, in order for the two-temperature model to correctly describe the interaction between ultrashort pulsed lasers and semiconductors, it is necessary to introduce a photoionisation equation describing the change in the density of free electrons on the basis of the two-temperature model[19]:

$$\frac{\partial N_e}{\partial t} = \nabla(D_e \nabla N_e) + \frac{\alpha}{h\nu} I + \frac{\beta}{2h\nu} I^2 - R_e \tag{1}$$

where N_e is the free electron density, D_e is the ambipolar diffusion coefficient, α is the single photon absorption coefficient, h is the Planck's constant, ν is the laser frequency, β is the two photon absorption coefficient, and the auger recombination electron rate R_e describes the rate of reduction of the free electrons induced by auger recombination as given in the following equation:

$$R_e = \frac{N_e}{\tau_r + \frac{1}{\gamma_R N_e^2}} \tag{2}$$

where $\tau_r$is the auger recombination time and γ_R is the auger recombination coefficient.

In the process of laser irradiation of diamond, the laser energy is Gaussian distributed in space, so the three-dimensional calculation region of the two-temperature equation can be simplified to a two-dimensional symmetric region, and because the depth of absorption of the laser energy in diamond is much smaller than the diameter of the laser spot, so it can be simplified from the two-dimensional region to a one-dimensional region, and the improved one-dimensional two-temperature model are shown below [15]:

$$C_e \frac{\partial}{\partial t} T_e = k_e \Delta^2 T_e - g(T_e - T_l) + S \tag{3}$$

$$C_l \frac{\partial}{\partial t} T_l = k_l \Delta^2 T_l + g(T_e - T_l) \tag{4}$$

$$C_e = \frac{3K_B N_e}{2} \tag{5}$$

$$k_e = \frac{v_e^2 \tau_e C_e}{3} \tag{6}$$

where C_e is the electron heat capacity, C_l is the lattice heat capacity, k_e is the electron thermal conductivity, v_e is electron velocity, τ_e is Electron–phonon coupling time.k_l is the lattice thermal conductivity, g is the electron - lattice coupling coefficient, and S is the laser-input heat source with the following equation:

$$S = \frac{\alpha I}{h\nu}(h\nu - E_g) + \frac{\beta I^2}{2h\nu}(2h\nu - E_g) \tag{7}$$

where E_g is the band gap energy of diamond and I is the laser intensity of the incident laser, the laser intensity is Gaussian distributed in time and space and follows the Beer-Lambert law in depth, the laser intensity is shown in Eq. (8):

$$I(t,z) = \frac{2F}{\sqrt{\pi/ln2}\,\tau_p}(1-R)\exp\left(-(4ln2)\frac{t^2}{\tau_p^2} - \int_0^z \alpha dz\right) \tag{8}$$

where F is the laser energy density, τ_p is the laser pulse width, and R is the reflectivity of the semiconductor surface to the laser.

Many studies have taken the reflectance R and absorption coefficient α in the two-temperature model as fixed values for the sake of calculation convenience, while a large number of studies have shown that the absorption coefficient and reflectance of the surface of the material changed with the increase of the free electron density during the laser processing of semiconductor materials [19]. In order to make the calculation results closer to the actual situation, we introduced the Drude model [20] to describe the optical properties of the free-electron gas to correct the surface reflectance. The Drude model can effectively show the relationship between the surface reflectivity of the material and the free electron density, and the complex dielectric coefficient of the diamond surface under the correction of the Drude model can be expressed as:

$$\varepsilon = \varepsilon_1 + i\varepsilon_2 = \left(1 - \frac{\omega_p^2 \tau_e^2}{1 + \omega^2 \tau_e^2}\right) + i\left(\frac{\omega_p^2 \tau_e}{\omega(1 + \omega^2 \tau_e^2)}\right) \tag{9}$$

where ε_1 and ε_2 are the real and imaginary parts of the complex dielectric coefficient ε, respectively, and ω_p is the plasma frequency:

$$\omega_p = \sqrt{\frac{N_e e^2}{m_e \varepsilon_0}} \qquad (10)$$

where m_e is the electron effective mass and ε_0 is the vacuum dielectric constant. The complex refractive index of the material $\tilde{n} = \sqrt{\varepsilon} = n + ik$, and the reflectance and absorption coefficient of the diamond surface can be expressed by the Fresnel expression as:

$$R = \frac{(n-1)^2 + k^2}{(n+1)^2 + k^2} \qquad (11)$$

$$\alpha = \frac{4\pi k}{\lambda} \qquad (12)$$

Then, the two-temperature model modified by the Drude model to account for changes in the optical properties of the material surface is achieved.

2.2 Molecular dynamics model

The molecular dynamics simulation can intuitively observe the microscopic changes of the material in a very short time. The process of picosecond laser ablation of CVD diamond was simulated by Lammps, and a one-dimensional laser ablation model was established, with a model volume of 10 nm × 10 nm × 400 nm, in which the volume of the CVD diamond was 10 nm × 10 nm × 200 nm and a vacuum region of 200 nm existed in the upper part of the diamond model. The length and width directions of the model were constrained by periodic boundary conditions, with free boundary conditions on the upper surface and absorbing boundary conditions on the lower surface. The micro-canonical ensemble(NVE) were used in the whole model region, and the interactions between carbon atoms were described by Tersoff potentials[21], and the simulation is set to have a time step of 1fs.

The simulation model consists of five parts: the vacuum layer, the laser absorption layer, the thermal conductivity layer, the constant temperature layer and the boundary layer. The vacuum layer allows the laser-abraded diamond to eject atoms and clusters into this region, the laser absorption layer is the main region where the diamond model absorbs the laser energy, the thermal conductivity layer is used to conduct further absorption and conduction of the heat transferred down from the absorption layer, and the thermostatic layer employs the boundary condition of energy absorption to simulate the infinite heat transfer process of the whole system by using the Langevin thermostatic heat bath, and the atoms inside the boundary layer are designated as ghost atoms, which are used to restrict the model to move in the negative direction of the z-axis. The simulation model of picosecond laser ablation of CVD diamond is shown in Fig. 1.

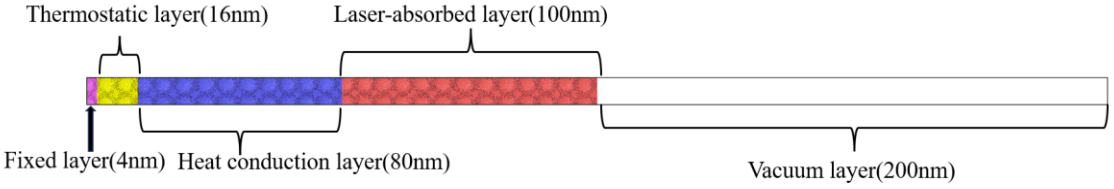

Fig.1. The diamond model of molecular dynamics

The simulation of picosecond laser ablation of CVD diamond requires an energy minimisation operation of the model to eliminate the irrational structures in the model, so the CVD diamond model was subjected to 20 ps of equilibrium relaxation process in the NVT system with a constant temperature of 300 K prior to the simulation.

Since molecular dynamics cannot describe the change of the free electron density of the material with time during the laser ablation process, the two-temperature model is coupled with molecular dynamics to perform molecular dynamics simulation of the model. Firstly, the two-temperature model is solved to obtain the energy transferred from electrons to the lattice during the electron-lattice chirp process of laser ablation of diamond, and then the laser absorbing layer in the molecular dynamics model of diamond is uniformly divided into 25 layers along the z-axis direction, and the energy obtained in the two-temperature model is inputted into the laser absorbing layer as a heat source to realise the coupling of the two-temperature model and molecular dynamics solution.

3. Simulation results and discussion

3.1 Simulation results for the two-temperature model

The change of free electron density during picosecond laser ablation of diamond was simulated by the photoionisation equation, and the evolution of free electron density with time is shown in Fig. 2(a). The free electron density increases continuously from 10 ps, when the laser energy density is low, single photon absorption is the main photoionisation mode, at this time the free electron density grows slowly; with the laser energy density increasing, the free electron density grows significantly faster, at this time two photon absorption is the main photoionisation mode. Afterwards, the free electron density increases slowly due to the change of surface reflectivity and absorption coefficient, and reaches the peak at 26 ps, after which the free electron density decreases to 3.5×10^{26}m^{-3}due to the decreasing energy density of the laser as well as the intermittent composite effect on the diamond surface.

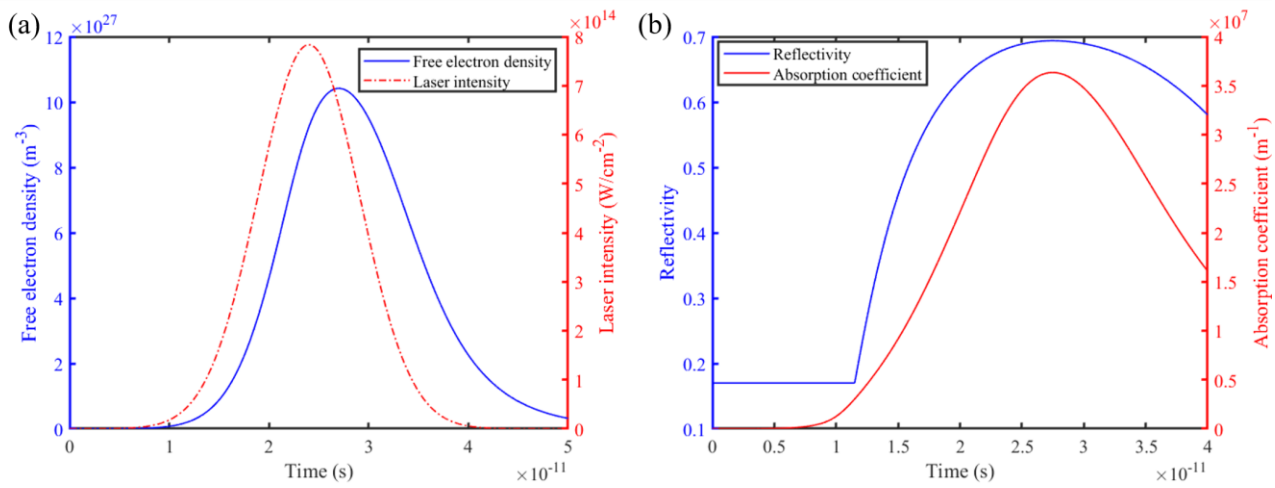

Fig.2. (a) Evolution of free electron density with time, (b) Evolution of reflectance and absorption coefficient with time; F=1 J/cm^2, τ_p=12ps, r=0μm, z=0μm

The time-dependent changes of the reflectance and absorption coefficient of the diamond surface during the laser ablation process were calculated by the drude model on the basis of the time-dependent changes of the free electron density, as shown in Fig. 2(b). The reflectance and absorption coefficient start from 1.2 ps and increase gradually with the increase of free electron density, and the reflectance of diamond surface reaches the maximum value of 0.69 at 25 ps, at which time the optical property of diamond surface has been transformed from a semiconductor to a metal, and quite a lot of energy will be reflected by the surface, so that the absorption coefficient of the surface decreases gradually.

The improved two-temperature model was solved by the finite-difference method, and the changes of electron temperature and lattice temperature with time are shown in Fig. 3. After the laser starts irradiating the diamond surface, the electron temperature of diamond starts to rise rapidly immediately, and with the increase of the laser energy density, the rising rate of the electron temperature also increases, and the electron-phonon chirp starts at 19 ps, and the electrons transfer the energy to the lattice through the electron-phonon chirp, and the temperature of the lattice starts to rise rapidly, and at the same time the rising rate of the electron temperature starts to decrease, and the electron temperature reaches the peak value of 3873K at 25 ps. The electron temperature reaches the peak value of 3873 K. The electron-phonon relaxation is completed at 60 ps, and the temperature reaches the equilibrium state, and the equilibrium temperature is 2905 K. The electron-phonon relaxation starts at 19 ps.

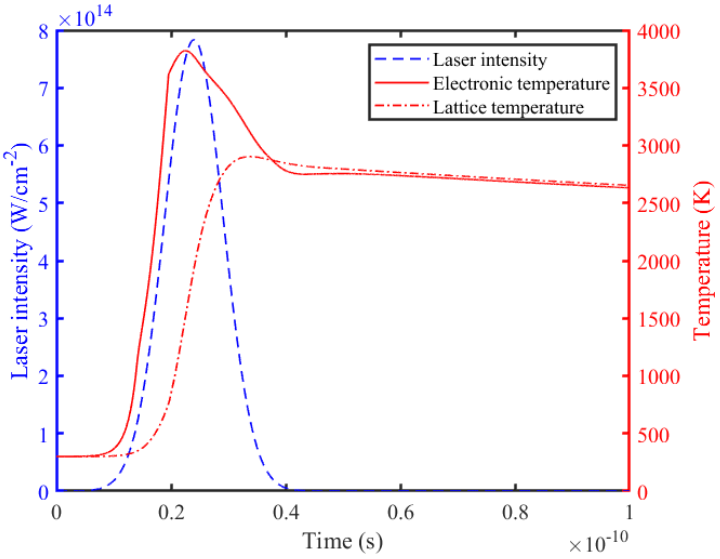

Fig.3. Evolution of electron temperature and lattice temperature with time; F=1 J/cm^2, τ_p=12ps, r=0μm, z=0μm

3.2 Simulation results for the molecular dynamics simulation

The molecular dynamics simulation of laser ablation of CVD diamond at different energy densities was carried out by the TTM-MD coupled model, and the simulation results are shown in Fig. 4, The blue parts of the figure represent diamond grains, the green parts represent diamond grain boundaries, and the white parts represent graphite and removed atoms:

(a) **F=1J/cm²**

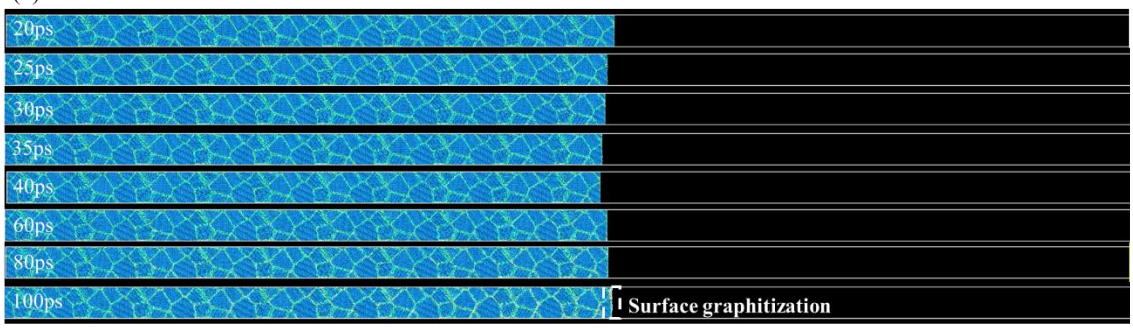

(b) **F=2.5J/cm²**

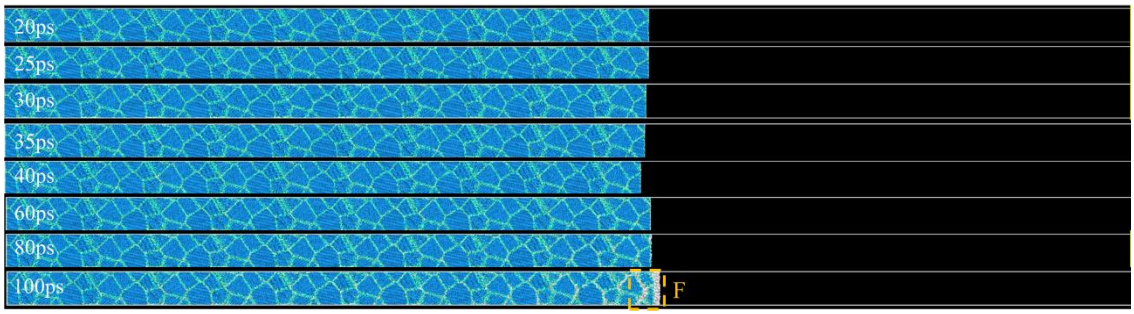

(c) **F=4.8J/cm²**

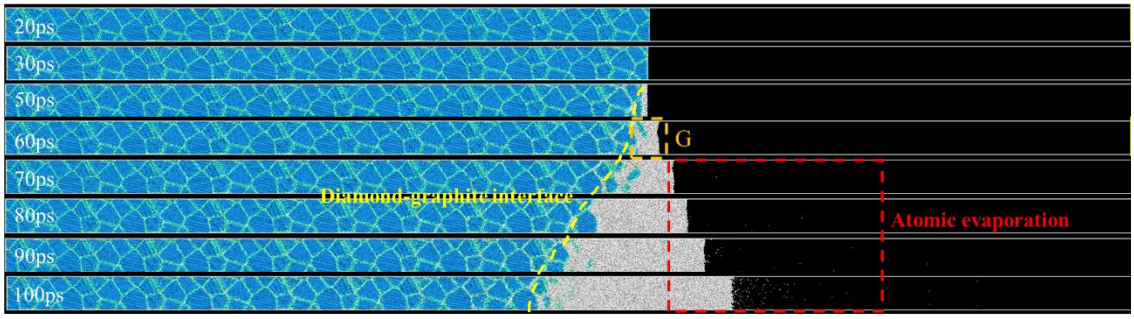

(d) **F=7J/cm²**

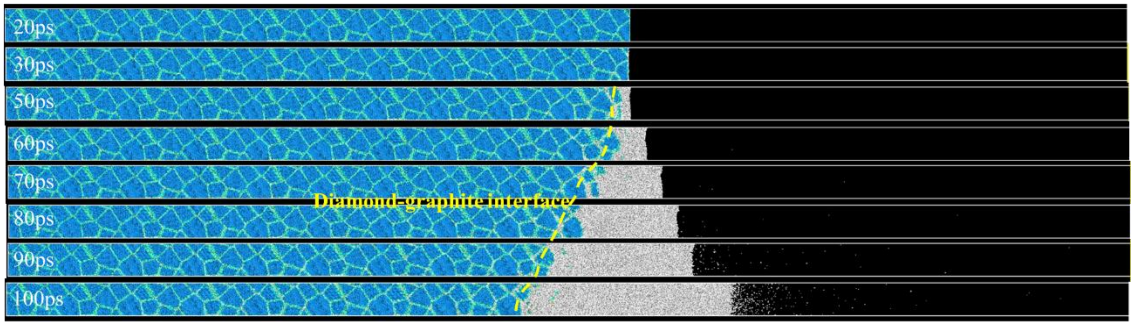

(e) **F=10J/cm²**

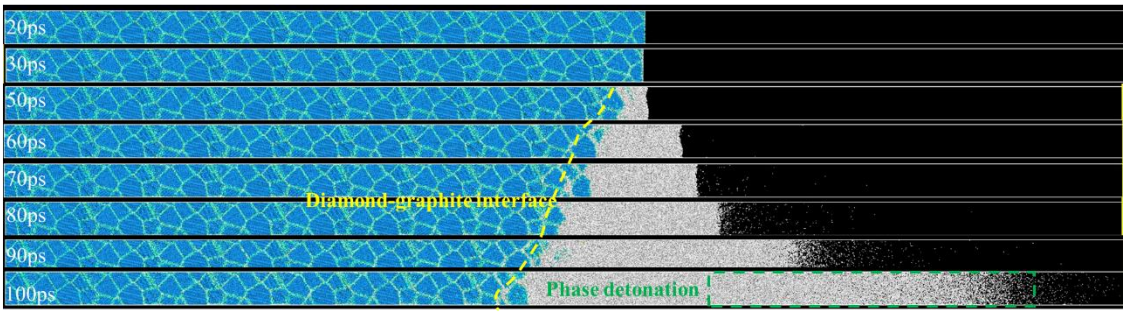

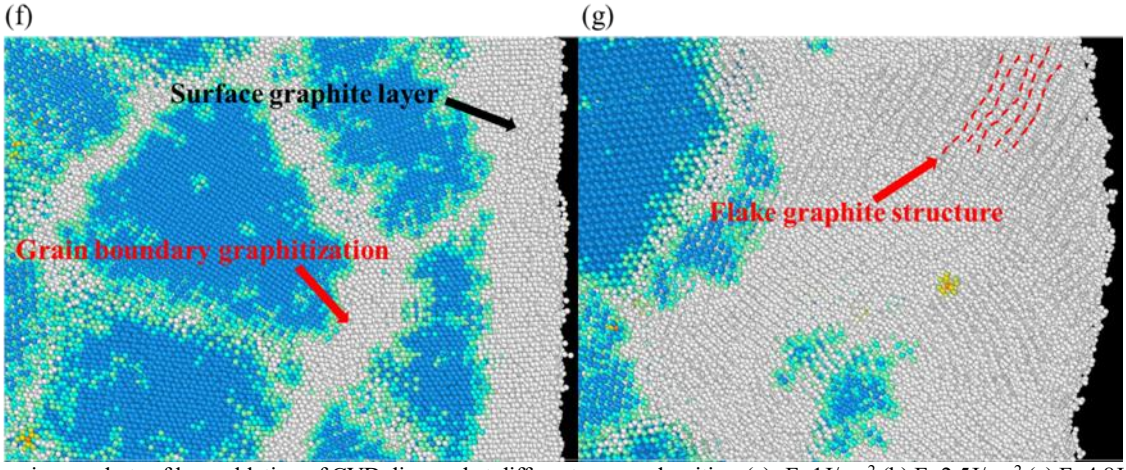

Fig. 4. Atomic snapshots of laser ablation of CVD diamond at different energy densities: (a) F=1J/cm^2,(b) F=2.5J/cm^2,(c) F=4.8J/cm^2,(d) F=7J/cm^2,(e) F=10J/cm^2, (f) Local magnified picture of Fig. 4b, (g) Local magnified picture of Fig. 4c

When the laser energy density is 1 J/cm^2 (Fig. 4a), the temperature of diamond increases under the irradiation of the laser and internal stresses are generated, causing the model to contract and then expand, and there is only slight graphitizing of diamond on the surface and no material removal occurs. When the laser energy density is 2.5 J/cm^2 (Fig. 4b), a graphite layer is formed on the diamond surface at the end of laser ablation, and at the same time graphitizing occurs at the diamond grain boundaries close to the surface, as shown in Fig. 4f. This is due to the fact that the atomic coordination number of the CVD diamond grains is 4, and the atomic coordination number of the grain boundaries is 3, which makes the potential at the grain boundaries higher than that at the grains, and the energy required for graphitizing to occur is smaller. Therefore, in the process of laser ablation of CVD diamond, the grain boundaries will be the first to be graphitized, forming a graphite layer wrapped around the grains, after which the grain boundaries will continue to expand and the grains will continue to shrink until they are completely graphitized. When the laser energy density is 4.8 J/cm^2 (Fig. 4c), with the loading of laser energy, the volume of the model gradually expands, and the depth of the graphite layer increases, and an obvious flake structure can be observed in the graphite layer part (Fig. 4g). 80 ps later, the surface of the model appears to be slightly ablated, and the material removal occurs in the form of atomic evaporation, and it can be regarded as the ablation threshold value of 4.8 for diamond. When the laser energy density is 7 J/cm^2 (Fig. 4d), the depth of the graphite layer of the model is further increased, and the ablation removal on the surface is more intense, and the removal is still in the form of atomic evaporation. When the laser energy density is 10 J/cm^2 (Fig. 4e), the model undergoes intense ablation removal, and the form of removal changes from atomic evaporation to phase explosion, and the form of removed particles changes from single atoms and small atomic clusters to a large number of large atomic clusters.

4. Ablation threshold test for CVD diamond

The ablation threshold test of picosecond laser ablation of CVD diamond was carried out, and the micro-morphology of laser ablation is shown in Figure 5. Due to the polycrystalline structure of CVD diamond, uneven removal of the diamond surface occurred after laser ablation. The grain boundaries between the diamond grains were removed before the grains are ablated, and pits are formed on the ablated surface, and graphite particles are produced in some areas. The diameters of ablation areas of diamond ablated by laser ablation under different powers were counted, the fitting curves of different ablation area diameters and laser energy density were plotted, and the single-pulse ablation threshold of picosecond laser ablation of CVD diamond was calculated by area extrapolation, which was 4.53J.

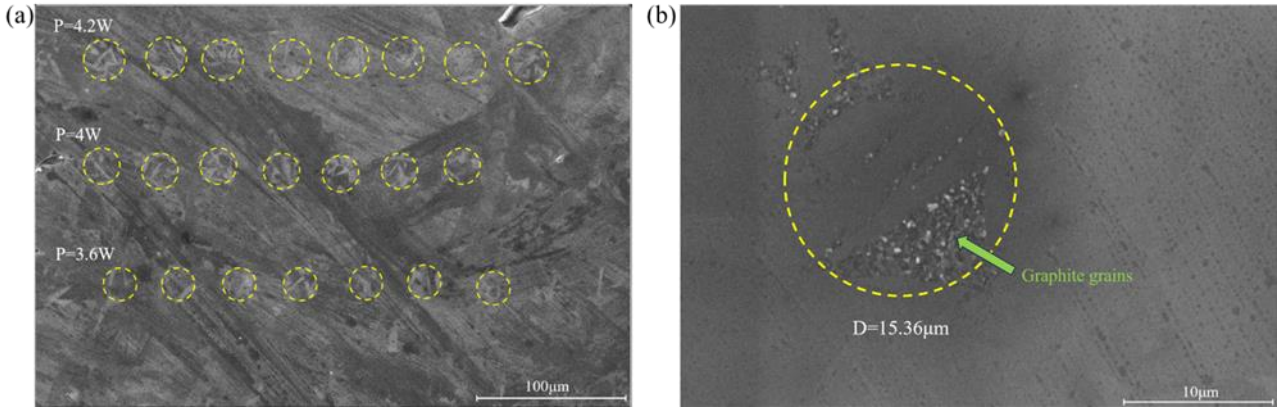

Fig. 5 (a) Scanning electron micrographs of laser ablated pits at different laser powers, (b) laser ablated area at a laser power of 4.2w

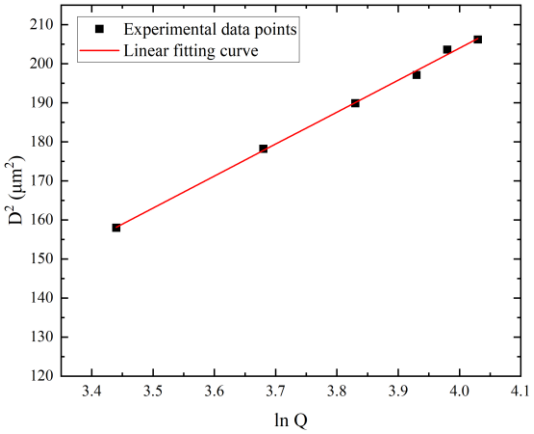

Fig. 6 Relationship between laser energy density and square of ablation pit diameter

5. Conclusion

In this paper, the two-temperature model is improved by taking the change of optical properties of diamond surface into consideration, and the TTM-MD model coupled with the two-temperature model and molecular dynamics is established, where the removal mechanism of CVD diamond by picosecond laser ablation is investigated by molecular dynamics simulation and the simulation model is verified by the ablation threshold test. The following conclusions can be drawn:

(1) With the increase of laser energy density, the thickness of the graphite layer produced on the surface of CVD diamond increases continuously, and the graphite layer firstly grew along the grain boundaries and surround the grains in the graphitization process of CVD diamond. The graphite layer at the grain boundaries became wider and the grains continued to shrink until completely graphitized.

(2) With the increase of laser energy density, the removal mode of CVD diamond changed from atomic evaporation to phase explosion, and the removal product changed from smaller atomic clusters to large atomic clusters.

(3) The ablation threshold of CVD diamond processed by picosecond laser with a pulse width of 12 ps is 4.53 J, and the ablation threshold obtained by the TTM-MD model is 4.8 J. The difference between the two is 5.62%, and the accuracy of the simulation model is verified.

References

[1] S.E. Coe, R.S. Sussmann, Optical, thermal and mechanical properties of CVD diamond, Diamond and Related Materials,9(9-10)(2000)1726-1729, https://doi.org/10.1016/S0925-9635(00)00298-3.

[2] Pontus Forsberg, Mikael Karlsson, High aspect ratio optical gratings in diamond, Diamond and Related Materials,34(2013)19-24, https://doi.org/10.1016/j.diamond.2013.01.009.

[3] Chris J.H. Wort, Richard S. Balmer, Diamond as an electronic material, Materials Today,11(1-2)(2008)22-28, https://doi.org/10.1016/S1369-7021(07)70349-8.

[4] Nicolas Mounet, Nicola Marzari, First-principles determination of the structural, vibrational and thermodynamic properties of diamond, graphite, and derivatives, Physical Review B,71(20)(2005)5241, https://doi.org/10.1103/PhysRevB.71.205214.

[5] Jialin Yang, Kewei Liu, Xing Chen, Dezhen Shen, Recent advances in optoelectronic and microelectronic devices based on ultrawide-bandgap semiconductors, Progress in Quantum Electronics,83(2022)100397, https://doi.org/10.1016/j.pquantelec.2022.100397.

[6] Sergey Terentyev, Vladimir Blank, Sergey Polyakov, Sergey Zholudev, Anatoly Snigirev, Parabolic single-crystal diamond lenses for coherent x-ray imaging, Applied Physics Letters,107(11)(2015)111108, https://doi.org/10.1063/1.4931357.

[7] Zongliang Cao, Dean Aslam, Fabrication technology for single-material MEMS using polycrystalline diamond, Diamond and Related Materials,19(10)(2010)1263-1272, https://doi.org/10.1016/j.diamond.2010.06.005.

[8] K.H Ho, S.T Newman, S Rahimifard, R.D Allen, State of the art in wire electrical discharge machining (WEDM), International Journal of Machine Tools and Manufacture,44(12-13)(2004)1247-1259, https://doi.org/10.1016/j.ijmachtools.2004.04.017.

[9] Markus Prieske, Markus Prieske, Picosecond-laser polishing of CVD-diamond coatings without graphite formation, Materials Today: Proceedings, 40(2021)1-4, https://doi.org/10.1016/j.matpr.2020.01.283.

[10] Zhen Zhang, Quanli Zhang, Jiuhua Xu, The crack propagation and surface formation mechanism of single crystalline diamond by a nanosecond pulsed laser, Journal of Applied Physics,130(11)(2021)1-15, https://doi.org/10.1063/5.0057163.

[11] Zhenjun Li, Ni Chen, Liang Li, Yang Wu, Ning He, Influence of the grain size of CVD diamond on the thermal conductivity, material removal depth and surface roughness in nanosecond laser machining, Ceramics International,14(12)(2020)20510-20520, https://doi.org/10.1016/j.ceramint.2020.05.157.

[12] Bakhtiar Ali, Han Xu, Robert T. Sang, Igor V. Litvinyuk, Maksym Rybachuk, Optimised diamond to graphite conversion via a metastable sp^1-bonded carbon chain formation under an ultra-short femtosecond (30 fs) laser irradiation, Carbon,204(2023)575-586, https://doi.org/10.1016/j.carbon.2023.01.012.

[13] S.I. Anisimov, B.L. Kapeliovich, T.L. Perelman, Electron emission from metal surfaces exposed to ultrashort laser pulses, Zhurnal ėksperimentalnoĭ i teoreticheskoĭ fiziki,66 (2) (1974)776–781.

[14] Lan Jiang, Hai-Lung Tsai, Improved Two-Temperature Model and Its Application in Ultrashort Laser Heating of Metal Films, Journal of Heat Transfer,127(10)(2005)1167-1173, https://doi.org/10.1115/1.2035113.

[15] Jiu Yin, Genyu Chen, Zhichao Zhu, Mengqi Jin, Bang Hu, Ablation mechanism investigation and ablation threshold prediction of single crystal diamond irradiated by femtosecond laser, Diamond and Related Materials,111(2021)108173, https://doi.org/10.1016/j.diamond.2020.108173.

[16] Xinrui Cui, Guo Li, Chunyu Zhang, Junjie Zhang, Liang Zhao, Molecular dynamics simulation of laser-induced graphitization of CVD diamond, Eighth Symposium on Novel Photoelectronic Detection Technology and Applications, 2022, 12169: 980-989, https://doi.org/10.1117/12.2623957.
[17] Boyu Tian, Wenbo Ma, Shifei Chen, Fanghong Sun, Xinchang Wang, Effects of pulsed laser processing on structural evolution of diamonds - A molecular dynamics and experimental study, International Journal of Refractory Metals and Hard Materials,119(0)(2024)106560, https://doi.org/10.1016/j.ijrmhm.2024.106560.
[18] Jian Liu, Mingtao Wu, Zhiyuan Sun, Quanli Zhang, Yandan Zhu, The picosecond laser ablation mechanism of monocrystalline silicon by coupling two-temperature model (TTM)-Molecular dynamic (MD), Applied Surface Science,661(2024)160022, https://doi.org/10.1016/j.apsusc.2024.160022.
[19] Hao Zhang, S. A. Wolbers, D. M. Krol, J. I. Dijkhuis, D. van Oosten, Modeling and experiments of self-reflectivity under femtosecond ablation conditions, Journal of the Optical Society of America B,32(4)(2015)606, https://doi.org/10.1364/JOSAB.32.000606.
[20] E.G. Gamaly, A.V. Rode, Physics of ultra-short laser interaction with matter: From phonon excitation to ultimate transformations, Progress in Quantum Electronics,37(5)(2013)215-323, https://doi.org/10.1016/j.pquantelec.2013.05.001.
[21] J. Tersoff, Empirical interatomic potential for carbon, with applications to amorphous carbon, Physical Review Letters,61(25)(1988), https://doi.org/10.1103/PhysRevLett.61.2879.